

Co(OH)₂/TiO₂ Nanotube Composite for High-Rate Performance Supercapacitor

Ren Xin¹, Qi Pengtao¹, Du Liang¹, Cheng Lili¹, Gao Zhiliang², Wang Ming^{1*}

¹College of Materials Science and Engineering, Liaoning Technical University, 47 Zhonghua Road, Fuxin 123000, Liaoning, China

²Zhucheng Aoling Automobile Factory of Shandong, Economic Development Zone, Zhucheng 262200, Shandong, China

*mwang.lntu@hotmail.com

Keywords: TiO₂ nanotubes; Co(OH)₂ nanoparticles; Electrochemical Properties; Supercapacitors

Abstract The TiO₂ nanotube arrays were prepared on Ti plate by anodizing technology, and then Co(OH)₂ nanoparticles in-situ grew into TiO₂ nanotubes with "Tube-particle bonding" nano-composited structure. Co(OH)₂ nanoparticles with a particle size of 40.5±8 nm were infiltrated in the TiO₂ nanotube arrays, and the Co(OH)₂ outside the tube presented a nanosheet structure. The specific capacitance of the Co(OH)₂/TiO₂ nanotube array composite reached 260 F/g at the current density ~1 A/g. The capacity retention rate was 82.5 % after 2000 cycles at the current density~5 A/g. The high-rate performance of the Co(OH)₂/TiO₂ nanotube array composite reached 210 F/g at the current density~10 A/g.

Introduction

Supercapacitors are widely used in the fields of portable electronic equipment, hybrid electric vehicles and national defense technology. Electrode materials become the most critical factor that will determine the performance of supercapacitors, which have also become the main aspect of supercapacitor study [1-4]. In general, pseudo capacitance electrode materials composed of transition metal oxides or conductive polymers have higher energy density than electric double layer capacitor electrode materials composed of carbon materials. Therefore, pseudo capacitance electrode materials have gradually become the main research topics [5-7].

Traditionally, active materials with pseudocapacitive properties are attached to conductive base materials (nickel foam) with adhesives (PTFE, PVDF) [8-10]. However, the binder generally reduces the conductivity of the electrode, hinders the transfer of electrons, and reduces the area accessible by the active material and the electrolyte [11-12]. The free-standing TiO₂ nanotube arrays have good chemical stabilities, large specific surface area and a highly ordered nanotube structure that can be used as a channel for charge transfer. This microstructure is beneficial to the rapid transfer of electrolyte ions at the electrode/electrolyte interface. The actual specific capacitance of Co(OH)₂ is severely smaller than the theoretical value [13-15].

In this work, the in-situ free-standing growth of TiO₂ nanotube arrays on the titanium sheet was prepared by anodizing method, and Co(OH)₂ nanoparticles were generated in-situ in the nanotubes. Co(OH)₂/TiO₂ nanotube array composite was successfully prepared. The electrochemical properties of the Co(OH)₂/TiO₂ nanotube array composite was tested.

Experimental

Pure metal titanium was wire-cut into 10×20×1.5mm thin slices and polishing. The TiO₂ nanotube arrays were prepared on Ti sheet using anodizing technology at 15 V and 1 h. The prepared TiO₂ nanotube arrays were put into 0.013 g/mL CoCl₂ aqueous solution and stirred well. Due to the small diameter of the TiO₂ nanotubes, the pressure inside the tube was so large that the natural deposition of active material cannot be infiltrated. Therefore, it was put into an ultrasonic instrument and subjected to ultrasound for 1 h to exhaust the air in the TiO₂ nanotube so that Co²⁺ could enter the

TiO₂ nanotube array. The deposited Co(OH)₂/TiO₂ nanotube arrays composite material were washed with distilled water, and then were dried at 60 °C to obtain the Co(OH)₂/TiO₂ nanotube composite.

The crystal structure of the composite was characterized by X-ray diffraction (Shimadzu XRD-6100, Japan). A scanning electron microscope (SEM, JEOL 7500F) was used to observe the surface microstructure of the composite. The electrochemical properties of all specimens were tested by the electrochemical workstation (Shanghai Chenhua CHI660E). Co(OH)₂/TiO₂ nanotube array composite was used as working electrode, platinum mesh (1cm×1cm) was used as counter electrode, and Hg/HgO electrode was used as reference electrode.

Results and Discussion

The crystal structure of Co(OH)₂/TiO₂ nanotube composite was analyzed by X-ray diffraction method. The titanium sheet that generated TiO₂ nanotube arrays after anodization was directly subjected to X-ray diffraction. Therefore, the diffraction peaks corresponding to Ti (102), (103) crystal planes appeared at 52.8° and 70.5°, respectively. At the same time, compared with the standard JCPDS card, a weak diffraction peak appeared at 20° was corresponding to TiO₂ (100) crystal plane. Obvious diffraction peaks appeared at 10.8°, 22.3°, and 59.6° corresponding to the crystal planes of α-Co(OH)₂ in (001), (002), (110). In particular, the diffraction peak of the (001) crystal plane of α-Co(OH)₂ is the most representative [16]. It indicates that Co(OH)₂/TiO₂ nanotube array composite with titanium sheet was prepared successfully.

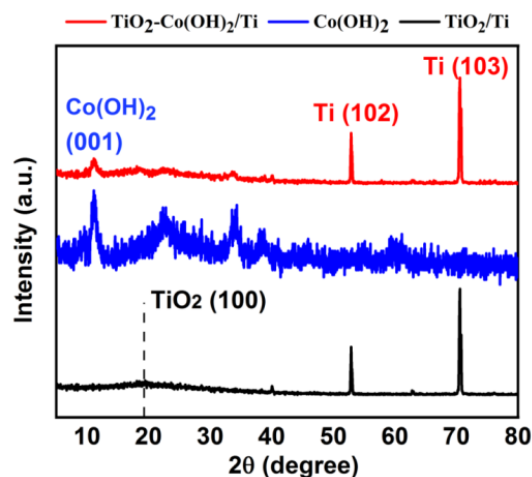


Fig.1 XRD patterns of different specimen of TiO₂, Co(OH)₂ and Co(OH)₂/TiO₂ nanotube composite

Figure 2 shows SEM images of TiO₂ nanotube, α-Co(OH)₂ and Co(OH)₂/TiO₂ nanotube composite. It can be seen that the TiO₂ nanotube arrays is neatly arranged and evenly distributed from Figure 2(a). The thickness of the tube wall was less than 10 nm. The average diameter of the nanotubes of the TiO₂ nanotube array was 43.6±8.2 nm. The α-Co(OH)₂ obtained by chemical deposition method (see Figure 2(b)) was a nanosheet layered structure, which was prone to stacking and agglomeration, causing a decrease in specific capacity [17-18]. It can be shown from Figure (c) that most of the TiO₂ nanotubes were loaded with loose α-Co(OH)₂ nanoparticles, and the size of the nanoparticles is 40.5±8 nm. α-Co(OH)₂ nanoparticles were embedded in the TiO₂ nanotube arrays to form a nanocomposite structure of "Tube-particle bonding". When the nanotube arrays were filled, the excess nanoparticles grew on the surface of the arrays to form a nanosheet structure, which it was clearer than pure α-Co(OH)₂ and also has a larger interlayer spacing and a thinner thickness. At the same time, there was no large-scale reunion. The composite material could fully contact more with electrolytes, which was more conducive to the improvement of electrochemical performance [19-20].

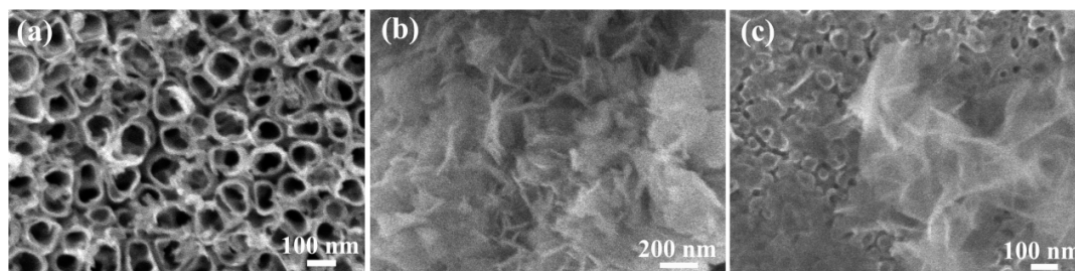


Fig.2 SEM images of different specimen. (a) TiO_2 nanotube arrays; (b) $\alpha\text{-Co(OH)}_2$; (c) $\text{Co(OH)}_2/\text{TiO}_2$ nanotube array composite

The prepared $\text{Co(OH)}_2/\text{TiO}_2$ nanotube composite was used as a supercapacitor material, and its specific capacitance was tested. The test results were shown in Figure 3(a) which is the constant current charge and discharge curve at a current density of 1 A/g. It could be obtained that the specific capacitance of the $\text{Co(OH)}_2/\text{TiO}_2$ nanotube array composite, TiO_2 nanotube and the $\alpha\text{-Co(OH)}_2$ was 260 F/g, 132 F/g and 140 F/g, respectively. The specific capacitance of the $\text{Co(OH)}_2/\text{TiO}_2$ nanotube composite reached nearly doubled compared with that of the original TiO_2 nanotube, and it was also significantly improved compared with the purer $\alpha\text{-Co(OH)}_2$, which was due to the TiO_2 nanotube arrays support the $\alpha\text{-Co(OH)}_2$ nanosheets and reduce agglomeration, so it was more conducive for the contact between the $\alpha\text{-Co(OH)}_2$ and the electrolyte and increased the specific capacitance of the composite. Figure 3(b) shows the constant current charge and discharge curves of $\text{Co(OH)}_2/\text{TiO}_2$ nanotube composite measured at current densities of 1, 2, 5, and 10 A/g, respectively. The corresponding specific capacitances were 260, 235, 218, 208 F/g. Compared with the specific capacitance at 1 A/g, the specific capacitance retention rate at 10 A/g current density reached 80%, which indicated the composite had higher rate performance. Figure 3(c) shows the capacity retention rate of $\text{Co(OH)}_2/\text{TiO}_2$ nanotube array composite and TiO_2 nanotube arrays under the current density of 5 A/g for 2000 cycles. It can be seen that the specific capacitance of the composite and TiO_2 gradually stabilized after 2000 cycles. The specific capacitance of the composite was retained to 82.5% compared with the initial specific capacitance and the specific capacity retention rate of the TiO_2 nanotube was only 72.7%. Therefore, the specific capacitance increased after $\alpha\text{-Co(OH)}_2$ was infiltrated, the composite exhibited better cycle stability. This was related to the $\alpha\text{-Co(OH)}_2$ nanoparticles in TiO_2 nanotubes that effectively exert electrochemical stability performance [21-22]. Figure 3(d) was the AC impedance spectrum of $\text{Co(OH)}_2/\text{TiO}_2$ nanotube composite compared with the pure $\alpha\text{-Co(OH)}_2$ and TiO_2 nanotube. In the high frequency region, the intercept between the curve and the abscissa represented the internal resistance R_s . The internal resistance of TiO_2 , $\alpha\text{-Co(OH)}_2$ and $\text{Co(OH)}_2/\text{TiO}_2$ nanotube composite was 0.52, 1.49, and 0.67 ohm, respectively. It can be seen that the internal resistance of the free-standing TiO_2 nanotube arrays were very low, and the insides of TiO_2 nanotube arrays can accelerate the movement of K^+ in the electrolyte, and the internal resistance did not change much after infiltrating $\alpha\text{-Co(OH)}_2$ nanoparticles. It showed that the $\alpha\text{-Co(OH)}_2$ nanoparticles and the TiO_2 nanotube walls were tightly bonded, which was consistent with the results of the microstructure (see Figure 2). In addition, the higher the slope of the line in the low frequency region was, the lower the ion diffusion resistance was. From Figure 3(d), the slopes of the $\text{Co(OH)}_2/\text{TiO}_2$ nanotube composite material and TiO_2 were similar, while the slope of $\alpha\text{-Co(OH)}_2$ was lower. It showed that the TiO_2 nanotube arrays in the composite have good conductivity, which improves the overall conductivity of the composite and promotes rapid electron transfer and rapid diffusion of electrolyte.

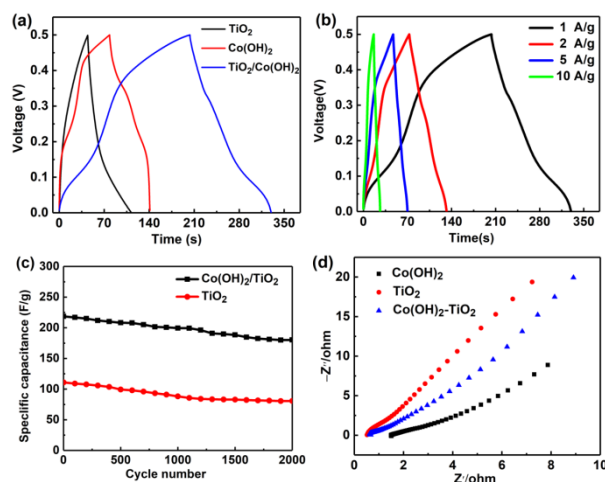


Fig.3 Electrochemical performance of different specimens. (a)Galvanostatic charge and discharge curve at current density of 1 A/g; (b)Galvanostatic charge and discharge curve at different rates; (c)Current density at 5 A/g long cycle; (d)Nyquist plots

Conclusion

In this paper, The microstructure and electrochemical performance of $\text{Co(OH)}_2/\text{TiO}_2$ nanotube composite were characterized and tested by XRD, SEM and electrochemical workstation, and the following were obtained in conclusion:

- 1) $\alpha\text{-Co(OH)}_2$ nanoparticles were embedded in the TiO_2 nanotube arrays to form a nanocomposite structure with "tube-particle bonding", and the composite was successfully prepared into a free-standing supercapacitor electrode material.
- 2) The specific capacitance of the $\text{Co(OH)}_2/\text{TiO}_2$ nanotube array composite was 260 F/g, which was nearly double the specific capacitance of the original TiO_2 nanotube. The specific capacitance retention rate was 80 % at a current density of 10 A/g, and it still had a capacitance retention rate of 82.5 % after 2000 cycles at a current density of 5 A/g. The $\text{Co(OH)}_2/\text{TiO}_2$ nanotube array composite showed a good electrochemical performance.

Acknowledgement

This work was supported that Science Research Foundation of Liaoning Province Education Department (LJ2020JCL027).

References

- [1] K. Malaie, M.R. Ganjali, Spinel nano-ferrites for aqueous supercapacitors; linking abundant resources and low-cost processes for sustainable energy storage, *J. Energy Storage*. (2020) 102097.
- [2] D. He, J. Wan, G. Liu, Design and construction of hierarchical $\alpha\text{-Co(OH)}_2$ -coated ultra-thin ZnO flower nanostructures on nickel foam for high performance supercapacitors, *J. Alloys Comp.* (2020) 155556.
- [3] D.P. Ojha, M.B. Poudel, H.J. Kim, Investigation of electrochemical performance of a high surface area mesoporous Mn doped TiO_2 nanoparticle for a supercapacitor, *Mater. Lett.* 264 (2020) 127363.
- [4] M. Wang, J.T. Huang, Research progress on synthesis and modification of $\text{Li}_4\text{Ti}_5\text{O}_{12}$ as Li-ion battery anode, *J. Func. Mater./Gongneng Cailiao*. 51 (2020) 03047.
- [5] S. Asim, M.S. Javed, S. Hussain, RuO_2 nanorods decorated CNTs grown carbon cloth as a free standing electrode for supercapacitor and lithium ion batteries, *Electro. Acta*. 326 (2019) 135009.

-
- [6] L. Zhang, Y. Tian, C. Song, Study on preparation and performance of flexible all-solid-state supercapacitor based on nitrogen-doped reduced graphene oxide/multi-walled carbon nanotubes/manganese dioxide, *J. Alloys Comp.* (2020) 157816.
- [7] M. Wang, H.X. Huang, P.T. Qi, Reduced grapheme oxide (RGO)/silicon network structured composites: preparation and electrochemical performance as anode materials for Li-ion batteries, *Mater. Reports*, 33 (2019) 927-931.
- [8] Y.H. Qu, X. Tong, C.H. Yan, Hierarchical binder-free MnO₂/TiO₂ composite nanostructure on flexible seed graphite felt for high-performance supercapacitors, *Vacuum*. 181 (2020) 109648.
- [9] N. Komba, G.X. Zhang, Z.H. Pu, MoS₂-supported on free-standing TiO₂-nanotubes for efficient hydrogen evolution reaction, *Inter. J. Hydro. Energy*. 45 (2020) 4468-4480.
- [10] J. Wang, Y.L. Liu, L. Cheng, Quasi-aligned nanorod arrays composed of Nickel–Cobalt nanoparticles anchored on TiO₂/C nanofiber arrays as free standing electrode for enzymeless glucose sensors, *J. Alloys Comp.* 821 (2020) 153510.
- [11] S. Noothongkaew, H.K. Jung, O. Thumtan, Synthesis of free-standing anatase TiO₂ membrane by using two-step anodization, *Mater. Lett.* 233 (2018) 153-157.
- [12] A. Ramadoss, S.J. Kim, Enhanced supercapacitor performance using hierarchical TiO₂ nanorod/Co(OH)₂ nanowall array electrodes, *Electro. Acta*. 136 (2014) 105-111.
- [13] H.N. Xing, Y.Y. Lan, Y. Zong, Ultrathin NiCo-layered double hydroxide nanosheets arrays vertically grown on Ni foam as binder-free high-performance supercapacitors, *Inorg. Chem. Commun.* 101 (2019) 125-129.
- [14] H. Li, Z.P. Sun, D.Z. Jia, Self-supporting TiO₂@NiCo₂S₄ arrays composite on the flexible Ti foil for a High-performance asymmetric supercapacitors, *Mater. Reports*. 34 (2020) 1187-1194.
- [15] M.N. Xu, H. Guo, R. Xue, Sandwich-like GO@Co(OH)₂/PANI derived from MOFs as high-performance electrode for supercapacitors, *J. Alloys Comp.* (2020) 157699.
- [16] C. Xu, Y. Chen, Y.N. Ma, Waste activated carbon transformed to electrode of supercapacitor through combining with Co(OH)₂, *Electro. Acta.* (2020) 137475.
- [17] J.T. Mehrabad, M. Aghazadeh, M.G. Maragheh, α -Co(OH)₂ nanoplates with excellent supercapacitive performance: electrochemical preparation and characterization, *Mater. Lett.* 184 (2016) 223-226.
- [18] M. Aghazadeh, K. Yavari, H.F. Rad, Oxygen-functionalized graphitic carbon nitride nanosheets/Co(OH)₂ nanoplates anchored onto porous substrate as a novel high-performance binder-free electrode for supercapacitors, *J. Energy Storage*. 32 (2020) 101743.
- [19] X. Li, L. Lu, J. Shen, Metal-organic frameworks induced robust layered Co(OH)₂ nanostructures for ultra-high stability hybrid supercapacitor electrodes in aqueous electrolyte, *J. Power Sources*. 477 (2020) 228974.
- [20] C.L. Wang, H.L. Qu, T. Peng, Large scale α -Co(OH)₂ needle arrays grown on carbon nanotube foams as free standing electrodes for supercapacitors, *Electro. Acta*. 191 (2016) 133-141.
- [21] M. He, W.L. Xu, Z.Q. Dong, Polyaniline hydrogel anchored in carbon cloth network to support Co(OH)₂ as flexible electrode for high-energy density supercapacitor, *Inorg. Chem. Commun.* 106 (2019) 158-164.
- [22] R. Rajagopal, K.S. Ryu, Homogeneous MnO₂@TiO₂ core-shell nanostructure for high performance supercapacitor and Li-ion battery applications, *J. Electroanal. Chem.* 856 (2020) 113669.